Robustness of Grazing-sliding Bifurcations in Hybrid Systems

Piotr Kowalczyk * **Jan Sieber** **

* *School of Mathematics, University of Manchester, Manchester, M13 9PL, U.K.*
** *Department of Mathematics, University of Portsmouth, Portsmouth, PO1 3HF, U.K.*

Abstract: In the paper we consider how orbits characterised by the presence of so-called sliding motion, which orbits typically occur in hybrid systems of *Filippov* type, are affected by stable singular perturbations. To be able to pursuit our analysis we consider a planar minimal system and we tune a system parameter such that a stable periodic orbit of the system touches the discontinuity surface: this is the so-called grazing-sliding bifurcation. We then check the effect of stable singular perturbation on the grazing cycle. In the unperturbed system the periodic orbit remains stable, and its local return map becomes piecewise linear. The effect of an arbitrarily small stable singular perturbation is that the local return map changes qualitatively, giving rise to, for example, period-adding cascades or small-scale chaos.

Keywords: Hybrid systems, chaos, robustness, grazing-sliding bifurcations.

1. INTRODUCTION

Recently much of research effort has been focused on analysis and control design of hybrid systems [Branicky (1996); Zhang et al. (2000); Lygeros (2005)], that is systems characterised by continuous and discrete evolution. A class of hybrid systems of our interest are so-called Filippov type systems, that is systems where the dynamics is governed by smooth vector fields in distinct domains of phase space. When so-called switching manifolds are reached by an evolving trajectory the systems switches from one vector field to another. Thus, the system trajectories are continuous but non-differentiable at the points where the aforementioned switchings take place.

In the simplest case we have two domains such that

$$\dot{x} = \begin{cases} f_-(x) & \text{if } h(x) < 0, \\ f_+(x) & \text{if } h(x) \geq 0. \end{cases} \tag{1}$$

The boundary between the domains is called the *switching manifold*: $\mathcal{H}_s = \{h(x) = 0\}$.

A special feature of Filippov systems is the so-called *sliding mode*, which means that a trajectory of the system does not follow any of the ODEs governing the domains but it rather 'slides' along the switching manifold, following a convex combination of the ODEs governing the adjacent domains:

$$\dot{x} = f_s(x) = \frac{[\partial h(x) f_-(x)] \cdot f_+(x) - [\partial h(x) f_+(x)] \cdot f_-(x)}{\partial h(x)[f_-(x) - f_+(x)]}. \tag{2}$$

Sliding occurs in all points x_0 of the switching manifold $\mathcal{H}_s$ where both vector fields point toward $\mathcal{H}_s$, that is, $\partial h(x) f_+(x) < 0$ and $\partial h(x) f_-(x) > 0$. Figure 1 illustrates the sliding evolution taking place along $\mathcal{H}_s$.

An important question for modelling is how sliding in a Filippov system is affected by perturbations. If we add a small perturbation to f_- or f_+ or to the switching decision h (the derivative of the perturbation is also assumed to be small) then any exponentially stable periodic orbit or equilibrium of a Filippov system persists [di Bernardo et al. (2007)] and remains stable. This also applies to pseudo-equilibria (equilibria of the sliding flow f_s, sitting exactly on the switching manifold) and to periodic orbits that have sliding segments. This persistence mirrors the results of classical bifurcation and invariant manifold theory for smooth dynamical systems [Fenichel (1979)].

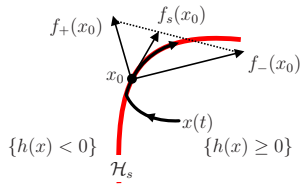

Fig. 1. A trajectory $x(t)$ through a point x_0 on the switching manifold $\mathcal{H}_s$ 'sliding' along $\mathcal{H}_s$ when the vector fields f_+ and f_- both point toward $\mathcal{H}_s$

Another typical perturbation arising in the modelling process are *stable singular* perturbations. In a simple model one replaces rapidly converging parts of the dynamics with their equilibrium, making the assumption that this equilibrium follows the slow dynamics *quasi-statically*. In a more complex model (or in reality) the equilibrium of the fast dynamics is not attained perfectly, which constitutes a small perturbation. Practical examples of this type of perturbation are small capacitances and inductances in electrical circuits, imperfect rigidity in mechanical systems, or fast chemical reactions (or other processes) in biological systems. Again, for smooth dynamical systems classical theory [Fenichel (1979)] proves that all hyperbolic equilibria, periodic orbits and, more generally, nor-

mally hyperbolic invariant manifolds persist. That is, for example, an exponentially stable equilibrium or periodic orbit (and any of its bifurcations) observed in a simple model obtained by making quasi-static assumptions is also present when the fast dynamics is taken into account as long as the difference in time scale is sufficiently large. In general, in smooth dynamical systems any phenomenon that persists under regular perturbations (perturbations of the right-hand-side) also persists under stable singular perturbations. The theoretical result [Fenichel (1979)] reduces hyperbolic singular perturbations to regular ones by proving the existence of a normally hyperbolic invariant manifold.

2. SINGULARLY PERTURBED FILIPPOV SYSTEMS

In order to find general statements how the dynamics and in particular the sliding type of motion in Filippov systems is affected by stable singular perturbations one has to study slow-fast systems of the form

$$\dot{x} = \begin{cases} f_-(x,y,\epsilon) & \text{if } h(x,y,\epsilon) < 0, \\ f_+(x,y,\epsilon) & \text{if } h(x,y,\epsilon) \geq 0, \end{cases} \tag{3}$$

$$\epsilon\dot{y} = g(x,y,\epsilon). \tag{4}$$

In system (3), (4) ϵ measures the difference in the time scales between the evolution of the slow variable x (usually vector valued) and the evolution of the fast variable y (in our case y is a scalar variable). We assume that for $\epsilon = 0$ the (then algebraic) equation (4) can be solved for y for all x, and that this solution $y_0(x)$ satisfies the stability condition

$$0 > -c > \text{Respec}\partial_2 g(x, y_0(x), 0) \tag{5}$$

with a uniform decay rate c. Condition (5) means that $y_0(x)$ is a locally exponentially stable equilibrium of the fast subsystem (4) if we treat the variable x in (4) as a parameter and set ϵ to 0 in the right-hand-side of (4).

Let us assume that the quasi-static approximation (called the *reduced* system from now)

$$\dot{x} = \begin{cases} f_-(x, y_0(x), 0) & \text{if } h(x, y_0(x), 0) < 0, \\ f_+(x, y_0(x), 0) & \text{if } h(x, y_0(x), 0) \geq 0 \end{cases} \tag{6}$$

has a stable periodic orbit $x(t)$ which is switching in $x_0 = x(t_0)$ from the subdomain $\{x : h(x, y_0(x), 0) \geq 0\}$ to sliding inside the manifold $\{x : h(x, y_0(x), 0) = 0\}$ (as shown in Figure 1). What happens to this periodic orbit if we include the singular perturbation effects by changing ϵ to a positive value?

3. MINIMAL EXAMPLE

To address this question we consider a system that admits an analytical expression for the local return map built around a periodic point of a periodic orbit. To this aim we use the Hopf normal form for f_+ combined with a constant vector field for f_- (the phase space dimension of the slow vector field is $n = 2$). We extend this two-dimensional system with an additional fast and stable scalar ODE for the variable y:

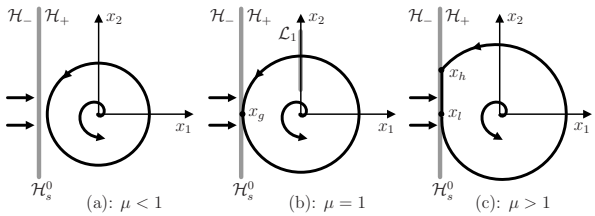

Fig. 2. Grazing-sliding scenario for the reduced system (9) of the minimal example. (a): the periodic orbit lies entirely in $\mathcal{H}_+$; (b): the periodic orbit touches the switching line $\{x_1 = -1\}$ at x_g; the line $\mathcal{P}$ is the Poincaré section chosen for the return map M_1 in (10); (c): the periodic orbit has a small sliding segment from x_h to x_l.

$$\dot{x} = \begin{cases} \begin{bmatrix} \mu x_1 - \omega x_2 - (x_1^2 + x_2^2)x_1 \\ \omega x_1 + \mu x_2 - (x_1^2 + x_2^2)x_2 \end{bmatrix} & \text{if } \theta x_1 + (1-\theta)y \geq -1 \\ \begin{bmatrix} 1 \\ 0 \end{bmatrix} & \text{if } \theta x_1 + (1-\theta)y < -1 \end{cases} \tag{7}$$

$$\epsilon\dot{y} = \epsilon\left[\mu x_1 - \omega x_2 - (x_1^2 + x_2^2)x_1\right] + x_1 - y \tag{8}$$

for $\theta < 1$.

The quasi-static approximation replaces y by $y_0(x, \mu) = x_1$ ($\epsilon = 0$ in (8)). Thus, the reduced model is

$$\dot{x} = \begin{cases} \begin{bmatrix} \mu x_1 - \omega x_2 - (x_1^2 + x_2^2)x_1 \\ \omega x_1 + \mu x_2 - (x_1^2 + x_2^2)x_2 \end{bmatrix} & \text{if } x_1 \geq -1 \\ \begin{bmatrix} 1 \\ 0 \end{bmatrix} & \text{if } x_1 < -1, \end{cases} \tag{9}$$

which is identical with the slow part (7). Only the switching function has changed to

$$h^0(x) = x_1 + 1.$$

For the reduced system (9) the flow in $\mathcal{H}_+ = \{h^0 \geq 0\}$ can be decomposed into a pair of uncoupled equations for the polar coordinates r and ϕ of $x \in \mathcal{R}^2$ ($x = r \cdot (\cos\phi, \sin\phi)$):

$$\dot{r} = \mu r - r^3, \qquad \dot{\phi} = \omega.$$

For $\mu > 0$ and $\omega \neq 0$ it has a unique stable periodic orbit corresponding to $r = \sqrt{\mu}$, $\phi = \omega t$ (a circle around the origin, see Figure 2(a)). This periodic orbit is also a periodic orbit of the reduced Filippov system (9) for $\mu < 1$. When we change μ to values larger than 1 the periodic orbit of the Filippov system (9) acquires a sliding segment starting from some point $x_h = [-1, x_{h,2}]^T$ ($x_{2,h} > 0$) and ending at $x_l = [-1, 0]^T$, making the overall orbit piecewise smooth (shown in Figure 2(c)): it has a corner at x_h and its second derivative is discontinuous at x_l. The periodic orbit is grazing the switching manifold $\mathcal{H}_s^0 = \{h^0 = 0\}$ for $\mu = 1$ as shown in Figure 2(b). This scenario is so-called grazing-sliding bifurcation. In the planar case considered here the effect of the grazing-sliding is an acquisition of a segment of sliding, and a discontinuous change in the value of the non-trivial Floquet multiplier corresponding to the periodic orbit, under the variation of μ through 1. For higher dimensional systems this scenario might lead to more complex dynamics, for instance to the sudden onset of chaos [di Bernardo et al. (2007)].

The point $x_g = [-1, 0]^T$ satisfies the conditions for a grazing-sliding event. Namely

- $h(x_g, y(x_g)) = 0$, (switching on the manifold $\mathcal{H}_s$ at x_g),
- $h_x f_+ = 0$, (grazing contact with $\mathcal{H}_s$ at x_g),
- $(h_x f_+)_x f_+ > 0$, (the grazing contact with $\mathcal{H}_s$ at x_g is quadratic),
- $(h_x + h_x g_x/g_y) f_+ > 0$ (the reduced vector field f_- points towards the switching surface);

subscripts denote differentiation with respect to indicated variables.

Let us now consider the local return map M_μ for the periodic orbit at $\mu = 1$ to the section $\mathcal{L}_1 = \{x : x_1 = 0, x_2 > 0\}$ (see Figure 2(b)). It has the form

$$M_1 x_2 = 1 + \begin{cases} \mathrm{e}^{-4\pi/\omega}[x_2 - 1] + O(|x_2 - 1|^2) & \text{if } x_2 < 1 \\ 0 & \text{if } x_2 \geq 1. \end{cases} \tag{10}$$

The map M_1 is piecewise asymptotically linear in its fixed point $x_2 = 1$ corresponding to the periodic orbit. For $\mu > 1$ the map M_μ is constant near its fixed point. In summary, in the reduced system (9) the only effect of the grazing-sliding bifurcation is that the periodic orbit changes its shape, and that its Floquet multiplier jumps from $\exp(-4\pi\mu/\omega)$ to 0 at the grazing parameter $\mu = 1$. The periodic orbit is stable for all $\mu \approx 1$. We will now study the system dynamics for $\varepsilon > 0$.

4. SLOW MANIFOLDS IN THE NEIGHBOURHOOD OF GRAZING

We have chosen the right-hand-side g of the fast equation (8) such that for $\epsilon > 0$ the subspace $\mathcal{M}_+ = \{(x, y) : x_1 = y\}$ is the exact slow invariant manifold of the flow E_+^t (following $\dot{x} = f_+$, $\epsilon\dot{y} = g$). That is, any trajectory will converge to $\mathcal{M}_+$ with a convergence rate of order ϵ^{-1} as long as it stays in the half space $\mathcal{H}_+ = \{(x, y) : \theta x_1 + (1 - \theta)y \geq -1\}$. The graph of the invariant manifold $\mathcal{M}_+$ is for all μ and ϵ

$$y_{m,+}(x) = x_1. \tag{11}$$

Since f_+ does not depend on y the *stable fibres* of the manifold $\mathcal{M}_+$ are: $\mathcal{F}_+(x_0) = \{(x, y) : x = x_0,\, y \in \mathcal{R}\}$ for all $x_0 \in \mathcal{R}^2$ (all points within a stable fibre converge to each other with a rate $O(\epsilon^{-1})$ following flow E_+^t forward in time). The graph of the slow invariant manifold $\mathcal{M}_-$ of E_- (the flow following $\dot{x} = f_-$, $\epsilon\dot{y} = g$) is not known analytically. Its expansion up to order ϵ is

$$y_{m,-}(x, \mu, \epsilon) = x_1 + \epsilon\left[\mu x_1 - \omega x_2 - (x_1^2 + x_2^2)x_1 - 1\right] + O(\epsilon^2). \tag{12}$$

The expressions for the slow invariant manifolds for E_+ and E_-, (11) and (12) differ from each other by a term of order ϵ (the difference is $\epsilon + O(\epsilon^2)$ for $x = (-1, 0)$, $y = -1$, $\mu = 1$, thus, it is non-zero at the grazing point). Hence, we expect that any trajectory crossing the switching manifold will show a small boundary layer; see Figure 3 for an illustration of the invariant manifolds $\mathcal{M}_\pm$ and the switching manifold $\mathcal{H}_s = \{(x, y) : \theta x_1 + (1 - \theta)y = -1\}$ near the grazing point at $\mu = 1$.

The switching manifold $\mathcal{H}_s$ for the example (7), (8) is a two-dimensional plane. Its intersection with the invariant manifold $\mathcal{M}_+$ is

$$\mathcal{H}_s \cap \mathcal{M}_+ = \{(x, y) : x_1 = y = -1\}.$$

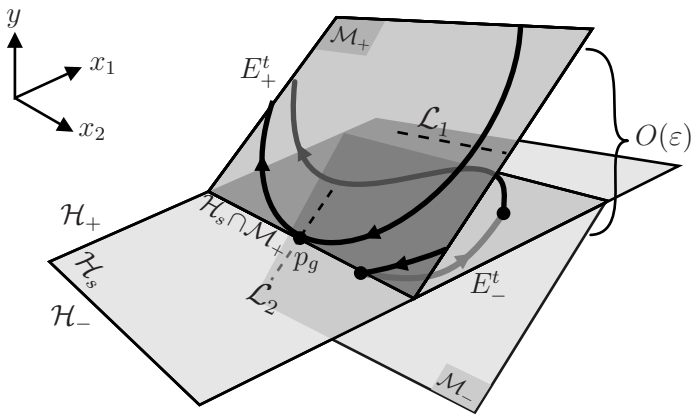

Fig. 3. Illustration of the manifolds near the grazing point p_g for the slow-fast example (7), (8) for $\epsilon > 0$, $\theta < 0$ and $\mu = 1$ (zoom-in near the grazing point p_g of the periodic orbit). The grazing periodic orbit lies entirely in $\mathcal{H}_+$ (and, thus, in$\mathcal{M}_+$). The other invariant manifold $\mathcal{M}_-$ (for $\mathcal{H}_-$) has a distance of $O(\epsilon)$ from $\mathcal{M}_+$. The illustration shows the grazing periodic orbit and a typical (for $\theta < 0$) switching trajectory near the periodic orbit, switching from E_+ to E_-, back to E_+, and then re-approaching $\mathcal{M}_+$.

5. DYNAMICS OF THE SYSTEM VIA RETURN MAPS

To be able to establish the dynamics around the grazing cycle of singularly perturbed system under consideration we construct the local return map around a periodic point of the grazing-cycle.To this aim we can proceed as follows. Let us derive an expression for the return map to the section $\Sigma_1 = \{(x, y) : x_1 = 0, x_2 > 0, y \in \mathcal{R}\}$ (which is away from the grazing point; see Figure 3 for $\mathcal{L}_1 = \Sigma_1 \cap \mathcal{M}_+$), more specifically the local return map to a small neighbourhood $\mathcal{U} \subset \Sigma_1$ of the point $(x, y)^T = (0, 1, 0)^T$, which is the fixed point at $\mu = 1$ corresponding to the grazing periodic orbit. Any trajectory starting in $\mathcal{U}$ spends a time of approximately $\pi/(2\omega)$ following E_+ before it reaches the vicinity of the switching manifold $\mathcal{H}_s$ in a small neighbourhood $\mathcal{V}$ of the point $p_g = (-1, 0, -1)^T$. During this time the difference between y and x_1 (which is the distance to the slow invariant manifold $\mathcal{M}_+$) decays such that $|y - x_1| \sim \exp(-\pi/(2\omega\epsilon))$ when the trajectory reaches $\mathcal{V}$, which is beyond all orders of ϵ. A trajectory leaving $\mathcal{V}$ follows E_+ for a time of approximately $3\pi/(2\omega)$ until it reaches Σ_1. Again, after this time the y-component and the x_1-component of the trajectory will be $\exp(-2\pi/(3\omega\epsilon))$ close. This means that the return map P is a one-dimensional map from the line $\mathcal{L}_1 = \Sigma_1 \cap \mathcal{M}_+ = \{(x, y) : x_1 = y = 0, x_2 > 0\}$ back to itself if we ignore terms of order $\exp(-c/\epsilon)$ where $c > 0$ is of order 1. It is a composition of four maps. Calling the time derivative of h with respect to each of the flows as $h'_\pm$, respectively,

$$h'_\pm(x, y) = \partial h(x, y) \frac{d}{dt} E_\pm^t(x, y)|_{t=0} = [\partial_1 h f_\pm + \epsilon^{-1} \partial_2 h g](x, y),$$

(dropping the argument ϵ) theses maps, say P_1 to P_4, can be described as follows

(1) P_1, maps from the line $\mathcal{L}_1 = \{x_1 = y = 0, x_2\} \cap \mathcal{U}$ to the curve $\mathcal{L}_2 = \{x_1 = y, h'_+(x,y) = 0\} \cap \mathcal{V}$ by following the flow E_+ within the slow invariant manifold $\mathcal{M}_+$ (see Fig. 3),
(2) P_2, the Poincaré-section discontinuity mapping from $\mathcal{L}_2$ to the plane $\Sigma = \{(x,y) : h'_+(x,y) = 0\} \cap \mathcal{V}$,
(3) P_3, maps from Σ back to $\mathcal{L}_2$, following the projection along the stable fibres of E_+: $P_3(x_1, x_2, y) = (x_1, x_2, x_1)$,
(4) P_4, maps from $\mathcal{L}_2 \subset \mathcal{V}$ back to $\mathcal{L}_1 \subset \mathcal{U}$ following E_+ inside the slow invariant manifold $\mathcal{M}_+$.

The character of the 'full' return map really depends on the character of P_2; P_2 is either piecewise affine or discontinuous with the discontinuity occurring at the point corresponding to the grazing periodic orbit. In the later case the map P_2 also contains a square root singularity on one side of the discontinuity. The type of the map P_2 and hence the dynamics of the system depends on the sign of the parameter θ. This parameter determines the intersection between the switching surface $\mathcal{H}_s$ and the slow manifolds $\mathcal{M}_\pm$.

In the case of $\theta < 0$ we observe the emergence of a repelling sliding region. That is we observe a creation of a region within $\mathcal{H}_s$ where the vector fields $f_\pm$ point away from $\mathcal{H}_s$ (this also implies a violation of one of the conditions for grazing-sliding at the grazing point).

To elucidate why P_2 can become discontinuous let us focus on Fig 3. There we depict a segment of the grazing cycle (that lives entirely on the slow manifold $\mathcal{M}_+$ and grazes the switching surface at p_g). Consider now a trajectory evolving in a sufficiently small neighbourhood of the grazing cycle which starts also on $\mathcal{M}_+$. After some time it reaches the switching surface at some point along the set $\mathcal{H}_s \cup \mathcal{M}_+$. In the standard grazing-sliding case any trajectory that evolves in sufficiently small neighbourhood of the grazing cycle and hits the switching surface is bound to follow the sliding motion for some non-zero time in the neighbourhood of the grazing point (p_g in our case). However, in the case depicted in Fig 3 the trajectory after reaching $\mathcal{H}_s \cup \mathcal{M}_+$ switches to vector field f_-– it does not follow sliding. This is due to the creation of the repelling sliding region in the neighbourhood of p_g. Then the trajectory reaches again the switching surface $\mathcal{H}_s$ before attaining the slow manifold $\mathcal{M}_-$. At this point the trajectory switches again to f_+ and moves towards the slow manifold $\mathcal{M}_+$. In this case the essential effect of the stable singular perturbation is the creation of the non-sliding evolution (evolution following f_-) in the neighbourhood of p_g This translates onto the character of the map P_2 – a discontinuous map captures the system dynamics. In the case of positive θ the theory of grazing-sliding bifurcations holds and the map is piecewise affine to leading order. However, another effect of the singular perturbation is that the map has non-zero slope for sliding trajectories and for instance an onset of chaotic motion can be observed in the system where the slow dynamics is two-dimensional.

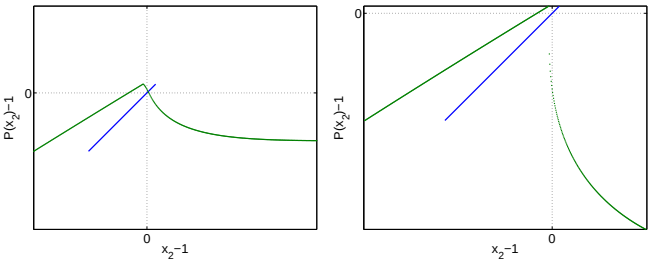

(a) $\theta = 0.5$ (b) $\theta = -0.5$

Fig. 4. Approximate local return map to $\mathcal{L}_1$, P, for $\epsilon = 0.01$, $\mu = 1 + \epsilon/2$, $\omega = 8\pi$ obtained numerically as the first return to $\mathcal{L}_1$ (neglecting the distance of the return point to $\mathcal{M}_+$; see Figure 3).

To summarise: in an appropriate co-ordinate set, for $\theta < 0$, the map P_2 can be given by

$$P_2(\tilde{x}_1) = \begin{cases} \tilde{x}_1 & \tilde{x}_1 \geq 0 \\ s_0 + \sqrt{\epsilon}(a\sqrt{-2\tilde{x}_1} + b(-2\tilde{x}_1)^{3/2}) + \mathcal{O}(\epsilon) & \tilde{x}_1 < 0 \end{cases},$$

where s_0, a and b are some constant; for $\theta > 0$, P_2 (to leading order in $\tilde{x}_1$) can be expressed as

$$P_2(\tilde{x}_1) = \begin{cases} \tilde{x}_1 & \tilde{x}_1 \geq 0 \\ A\tilde{x}_1 & \tilde{x}_1 < 0 \end{cases}$$

where A is some constant. For a detailed derivation of P_2 we refer to [Sieber and Kowalczyk (2008)].

In Fig. 4 we present a local return map around a grazing-sliding cycle from a section $\mathcal{L}_1$ back to itself. Indeed we observe that the graph is continuous for θ positive and discontinuous for negative θ. Piecewise discontinuous maps characterised by square root singularity on one side, among other dynamics outcomes, exhibit for instance inverse period adding cascades. In fig .5 we present different phase portraits of the slow-fast system (7) for $\mu \approx 1$. Under increasing μ through $\mu = 1$ we observe an inverse period-adding cascade. In Fig. 5(a) for $\mu = 1.001$ we can see a stable orbit of period-8. Increasing μ leads to a series of bifurcations that decrease the period of the orbit. We observe a period-5 orbit at $\mu = 1.01$ (In Fig. 5(b)) and a period-3 orbit at $\mu = 1.05$ (In Fig. 5(c)-(d)).

6. CONCLUSIONS

Stable singular perturbations have a much stronger influence on the dynamics in Filippov systems than in smooth dynamical systems. In the paper we have studied periodic orbits with an infinitesimally small sliding segment that is close to a grazing-sliding bifurcation. We found two generic cases depending on the geometry: the local return map around the grazing periodic orbit develops a discontinuity if the condition on the existence of an attracting sliding region is violated. Otherwise, the continuity of the return map persists but the asymptotic slope may have a change of order 1.

The qualitative change of the local return map induces qualitative changes to the dynamics on a small scale. A piecewise discontinuous map with a square-root singularity of the slope on one side of the discontinuity, as occurs for

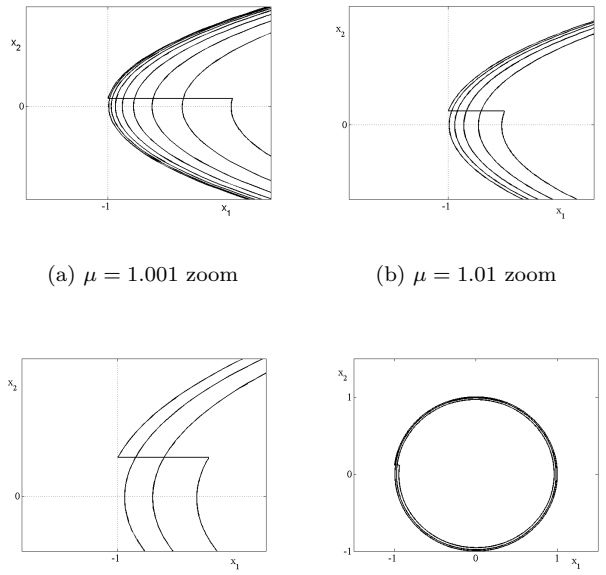

(a) $\mu = 1.001$ zoom (b) $\mu = 1.01$ zoom

(c) $\mu = 1.05$ zoom (d) $\mu = 1.05$

Fig. 5. Periodic orbits of the slow-fast system (7) for $\omega = 8\pi$, $\theta = -0.5$ and $\epsilon = 0.01$ in projection on the (x_1, x_2) plane. In Fig (a) to (c) only zoom in the neighbourhood of the switching surface is depicted

$\theta < 0$ in the minimal example, shows inverted period-adding cascades of periodic orbits if one varies the parameter μ through its critical value [Dutta and Banerjee (2008)]. The parameter range where these cascades can be observed is of order ϵ. In the other case, $\theta > 0$, the observed dynamics depends strongly on the one-sided derivative A. It can be chaotic if $A < -1$, which is possible for small θ.

The results presented can be generalised to higher-dimensional slow-fast systems in a straightforward manner as long as the dimension of the fast subsystem is 1. There are, however, some technical difficulties to generalising our finding for higher dimensional fast subsystems ($y \in \mathcal{R}^m$, $m > 1$).

The small-scale instabilities described in our paper might account for discrepancies between dynamics of systems with discontinuous nonlinearities that have been observed experimentally, and the numerical results of the models. See [Banerjee and Verghese (2001); Virgin and Begely (1999)] for examples relevant to engineering applications.

ACKNOWLEDGEMENTS

Piotr Kowalczyk would like to acknowledge EPSRC grant EP/E050441/1.

REFERENCES

Banerjee, S. and Verghese, G. (2001). *Nonlinear Phenomena in Power Electronics*. IEEE press, New York.

Branicky, M. (1996). Studies in hybrid systems: modeling, analysis, and control. Technical report, Massachusetts Institute of Technology.

di Bernardo, M., Budd, C., Champneys, A., and Kowalczyk, P. (2007). *Piecewise-smooth Dynamical Systems — Theory and Applications*, volume 163 of *Applied Mathematical Sciences*. Springer-Verlag.

Dutta, P. and Banerjee, S. (2008). Period increment cascades in a discontinuous map with square-root singularity. *Preprint*.

Fenichel, N. (1979). Geometric singular perturbation theory for ordinary differential equations. *Journal of Differential Equations*, 31, 53–98.

Lygeros, J. (2005). An overview of hybrid systems control. *Handbook of Networked and Embedded Control Systems*, 519–538.

Sieber, J. and Kowalczyk, P. (2008). Small-scale instabilities in dynamical systems with sliding. Submitted for publication to Physica D, November 2008.

Virgin, L.N. and Begely, C.J. (1999). Grazing bifurcations and basins of attraction in an impact friction oscillator. *Physica D*, 130, 43–57.

Zhang, J., Johansson, K., Lygeros, J., and Sastry, S. (2000). Dynamical systems revisited: Hybrid systems with zeno executions. In *HSCC*, 451–464.